Thermal Photon Radiation in High Multiplicity $p + \mathrm{Pb}$ Collisions at the Large Hadron Collider

Chun Shen,[1] Jean-François Paquet,[1] Gabriel S. Denicol,[1,2] Sangyong Jeon,[1] and Charles Gale[1]
[1]Department of Physics, McGill University, 3600 University Street, Montreal, Quebec H3A 2T8, Canada
[2]Physics Department, Brookhaven National Laboratory, Upton, New York 11973, USA
(Received 8 May 2015; published 18 February 2016)

The collective behavior of hadronic particles has been observed in high multiplicity proton-lead collisions at the Large Hadron Collider, as well as in deuteron-gold collisions at the Relativistic Heavy-Ion Collider. In this work we present the first calculation, in the hydrodynamic framework, of thermal photon radiation from such small collision systems. Owing to their compact size, these systems can reach temperatures comparable to those in central nucleus-nucleus collisions. The thermal photons can thus shine over the prompt background, and increase the low p_T direct photon spectrum by a factor of 2–3 in 0%–1% $p + \mathrm{Pb}$ collisions at 5.02 TeV. This thermal photon enhancement can therefore serve as a signature of the existence of a hot quark-gluon plasma during the evolution of these small collision systems, as well as validate hydrodynamic behavior in small systems.

DOI: 10.1103/PhysRevLett.116.072301

Introduction.—The experimental heavy-ion collision program conducted at the Relativistic Heavy-Ion Collider (RHIC) and the Large Hadron Collider (LHC) aims to create and study the quark-gluon plasma (QGP), a new phase of nuclear matter. Relativistic hydrodynamics is the standard theoretical framework used to describe the dynamical evolution of QGP created in ultrarelativistic heavy ion collisions; fluid-dynamical modeling has been very successful in describing a wide variety of measurements made at RHIC and the LHC. Through combined theoretical and experimental efforts, it was shown that the QGP produced at RHIC and LHC behaves as a strongly coupled fluid, with one of the smallest shear viscosity to entropy density ratios ever observed [1,2].

Nevertheless, the applicability of relativistic hydrodynamics has its limits; this theory is only valid in systems where the separation between microscopic and macroscopic distance or time scales is sufficiently large. This is expected to be the case in central through midperipheral ultrarelativistic heavy ion collisions, where the energies reached are high enough to produce the QGP and the volume is large enough to ensure that the system approaches the thermodynamic limit. However, it is not clear that this will be the case in proton-nucleus and proton-proton collisions, where QCD matter is produced in considerably smaller volumes.

Recently, signatures usually associated with hydrodynamic behavior have also been observed in high multiplicity $p + \mathrm{Pb}$ collisions at the LHC [3–5] and $d + \mathrm{Au}$ collisions at the RHIC [6]. In particular, multiparticle correlations among the produced hadrons (usually associated with collectivity) [7] and mass ordering of the identified particle elliptic flow coefficient (usually associated with radial flow) [8–10], were observed in the $p + \mathrm{Pb}$ collisions at the LHC. This came as a surprise, as such systems were believed to be too small to produce a strongly interacting fluid. The possibility that the QGP can also be produced in such small systems is currently a topic of intense debate in the field.

However, even though the above signals strongly support the fluid-dynamical nature of high multiplicity $p + \mathrm{Pb}$ and $d + \mathrm{Au}$ collisions, they do not yet represent concrete proof. In order to reach more concrete conclusions, one must first disentangle the initial-state [11–14] and final-state effects [15–20] in the observed collective phenomena—something that poses a great challenge from both the theoretical and experimental points of view.

Electromagnetic (EM) radiation from the QCD matter created in heavy-ion collisions is recognized as a clean penetrating probe [21] and can help clarify this situation. Photons suffer a negligible final state interaction once they are produced and therefore carry valuable dynamical information from their point of emission. At low transverse momentum, a direct photon signal that is much larger than the expected prompt photon background has been measured by PHENIX [22] in 200 GeV $\mathrm{Au} + \mathrm{Au}$ collisions and by the ALICE collaboration in 2760 GeV $\mathrm{Pb} + \mathrm{Pb}$ collisions [23]. The direct photons were found to have an elliptic flow (v_2) [24–27] as large as that of pions. These measurements have stimulated considerable theoretical effort in photon rate calculations [28–32] as well as in setting stricter constraints on the dynamical description of the medium evolution in heavy-ion collisions [33–42].

In this Letter we calculate, for the first time, the thermal photon radiation of a small and rapidly expanding QGP droplet. We find a significant yield of direct photons originating from thermal production in high multiplicity $p + \mathrm{Pb}$ collisions, which can serve as a clean signal of the

existence of a hot QGP medium in these collisions. We also consider measurements in minimum bias $p+\mathrm{Pb}$ and $d+\mathrm{Au}$ collisions at the LHC and RHIC and show that even in these cases one can see a sizable signal due to thermal radiation. Finally, we calculate the anisotropic flow $v_{2,3}\{\mathrm{SP}\}$ of direct photons in high multiplicity $p+A$ collisions and find that it is of the same magnitude as the one calculated in central $\mathrm{Pb}+\mathrm{Pb}$ collisions. The measurement of the direct photon $v_{2,3}\{\mathrm{SP}\}$ can further constrain the dynamical evolution of these small systems and helps us to extract the transport properties of a QGP droplet.

Model and calculation.—The event-by-event simulations employ the public code package iEBE-VISHNU [43], with initial conditions generated from the Monte Carlo Glauber (MCGlb) model. In this implementation of the MCGlb model, the entropy in the transverse plane is distributed by summing over 2D Gaussian profiles centered at the location of each participant. The width of the Gaussian profiles is $r=\sqrt{\sigma_{\mathrm{NN}}/8\pi}$, where σ_{NN} is the nucleon-nucleon inelastic cross section, and the amount of entropy deposited by each participant fluctuates according to a Gamma distribution. The overall entropy normalization is fixed by fitting the observed multiplicity of charged hadrons at midrapidity. Further details of the hydrodynamic model employed as well as of the MCGlb model can be found in Ref. [43]. Note that this prescription can describe the multiplicity distribution of charged hadrons measured in the $p+\mathrm{Pb}$ collisions at 5.02 TeV [44]. Realistic distributions of nucleons are used when sampling nuclei. The positions of the proton and neutron composing the deuteron are sampled using the Hulthen wave function [45], as outlined in Refs. [46,47]. For Au and Pb nuclei, the configurations calculated in Refs. [48,49] are used as input.

The produced initial density profiles are evolved using the viscous $(2+1)$-d hydrodynamic code VISH2+1 [50] with the lattice-based equation of state (EOS) `s95p-v0-PCE165` [51]. A constant shear viscosity to entropy ratio $\eta/s=0.08$ for $T>180$ MeV is assumed. For $T<180$ MeV, we use the parameterization [52]:

$$\frac{\eta}{s}(T)=0.681-0.0594\frac{T}{T_c}-0.544\left(\frac{T}{T_c}\right)^2. \quad (1)$$

Any preequilibrium dynamics is neglected, and it is assumed that the fluid is at rest in the transverse plane when the hydrodynamic evolution begins at $\tau_0=0.6$ fm. Owing to the fireball compact size, proton-nucleus collisions have larger initial pressure gradients than $A+A$ collisions. Those gradients drive a large expansion rate, and consequently lead to a strong hydrodynamic radial flow.

The applicability of fluid dynamics can be characterized by the Knudsen number [53],

$$K_\theta \equiv \tau_\pi\theta=\frac{5\eta}{e+\mathcal{P}}(\partial\cdot u), \quad (2)$$

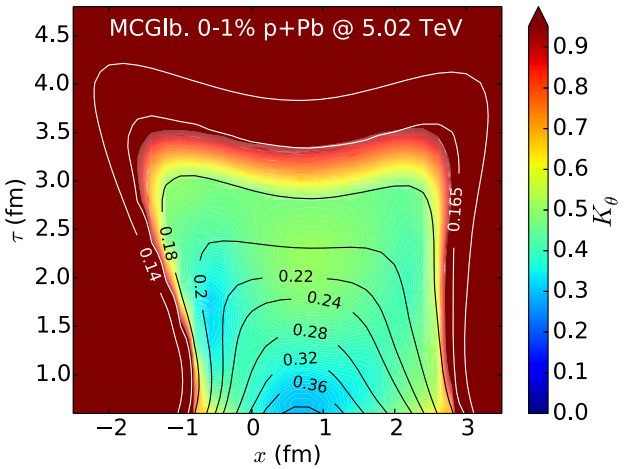

FIG. 1. Color contour plot for the space-time evolution of the Knudsen number, $K_\theta=\tau_\pi\theta$, in 0%–1% $p+\mathrm{Pb}$ collisions at 5.02 TeV. Constant temperature contours are shown.

with small values of Knudsen number ($K_\theta \ll 1$) supporting the validity of a hydrodynamic description. Figure 1 shows the Knudsen number of a typical ultracentral proton-nucleus collision. Its hydrodynamic description gradually breaks down as the temperatures decreases and, one can see that, for temperatures $T\lesssim 0.165$ MeV, the Knudsen number is already above one in almost all space-time points. For this reason, a kinetic freeze-out temperature $T_{\mathrm{dec}}=165$ MeV is used for the calculations that yield the results on which we report here. The thermal photon radiation is computed from the medium only above T_{dec}.

In the QGP phase, we use the full leading order $O(\alpha_s\alpha_{\mathrm{EM}})$ photon production rate [54]. In the hadron gas phase, photon production from mesonic channels [55], ρ spectral function, and $\pi+\pi$ bremsstrahlung [31] are taken into account. Shear viscous corrections are included in the 2 to 2 scattering processes in the QGP phase [30] and in all the mesonic reactions in hadron gas phase [28]. We switch rates from QGP to hadron gas at $T=180$ MeV, where the equilibrium rates from both phases are approximately the same [56].

The emitted thermal photon momentum distribution is computed by folding the thermal photon production rates, $q(dR/d^3q)(q,T)$, with the dynamically evolving medium, event by event [41]:

$$E\frac{dN^{\mathrm{th},\gamma}}{d^3p}=\int d^4x\left(q\frac{dR}{d^3q}(q,T(x),\pi^{\mu\nu}(x))\right)\Big|_{q=p\cdot u(x)}. \quad (3)$$

The anisotropic flow coefficients of the direct photons are calculated by correlating them with all charged hadrons, known as the scalar-product method [39],

TABLE I. Global hadronic observables in $p+\mathrm{Pb}$ collisions at 5.02 TeV and $d+\mathrm{Au}$ collisions at 200 GeV. The charged hadron anisotropic flow coefficients $v_{2,3}^{\mathrm{ch}}\{2\}$ are integrated from 0.3 to 3.0 GeV. The number of binary collisions within the given centrality bin is estimated using the Monte Carlo Glauber model.

$p+\mathrm{Pb}$ @ 5.02 TeV	$\langle N_{\mathrm{coll}}\rangle$	$(dN^{\mathrm{ch}}/d\eta)\vert_{\vert\eta\vert<0.5}$	$\langle p_T\rangle(\pi^+)$ (GeV)	$v_2^{\mathrm{ch}}\{2\}$	$v_3^{\mathrm{ch}}\{2\}$
0%–1%	15.4 ± 0.03	57.6 ± 0.3	0.59 ± 0.01	0.056 ± 0.001	0.018 ± 0.001
0%–100%	6.6 ± 0.01	16.6 ± 0.3	0.51 ± 0.02	0.034 ± 0.001	0.007 ± 0.001
$d+\mathrm{Au}$ @ 200 GeV	$\langle N_{\mathrm{coll}}\rangle$	$(dN^{\mathrm{ch}}/d\eta)\vert_{\vert\eta\vert<0.5}$	$\langle p_T\rangle(\pi^+)$ (GeV)	$v_2^{\mathrm{ch}}\{2\}$	$v_3^{\mathrm{ch}}\{2\}$
0%–100%	8.05 ± 0.01	8.85 ± 0.19	0.46 ± 0.02	0.025 ± 0.001	0.003 ± 0.001

$$v_n\{\mathrm{SP}\}(p_T) = \frac{\langle \frac{dN^\gamma}{dp_T} v_n^\gamma(p_T) v_n^{\mathrm{ch}} \cos[n(\Psi_n^\gamma(p_T) - \Psi_n^{\mathrm{ch}})]\rangle}{\langle \frac{dN^\gamma}{dp_T}\rangle v_n^{\mathrm{ch}}\{2\}}. \quad (4)$$

Table I summarizes the global hadronic observables from our simulations for $p+\mathrm{Pb}$ collisions at 5.02 TeV and $d+\mathrm{Au}$ collisions at 200 GeV. The MCGlb model with multiplicity fluctuations can correctly reproduce the centrality dependence of charged hadron multiplicity. For $p+\mathrm{Pb}$ collisions, the mean p_T of pions calculated is around 10% higher than the values experimentally observed [57]. The inclusion of bulk viscosity may reduce this tension with the data [58]. The charged hadron anisotropic flow coefficients, $v_{2,3}\{2\}$ for $p+\mathrm{Pb}$ collisions, are in reasonable agreement with the experimental measurements from the CMS collaboration [44], with $v_2\{2\}$ being slightly underestimated by the calculation.

Results and discussion.—Whether thermal photons can be observed or not depends on their contribution relative to prompt photons. In this Letter the prompt photon background is evaluated with perturbative QCD (pQCD) at next-to-leading order (NLO) [59–61], scaled with the number of binary collisions as computed in the Glauber model. For nucleus collisions, cold nuclear effects are included by using EPS09 nuclear parton distribution functions [62]. The isospin effect is included as well. The proton parton distribution function used is CTEQ6.1M [63] and the photon fragmentation function is BFG-2 [64]. The factorization, renormalization, and fragmentation scales are set equal to αp_T, where p_T is the transverse momentum of the produced photon. The constant α is set to $1/2$ so as to provide a good description of the available direct photon measurements at RHIC [65]. The minimum scale Q parametrized in the parton distribution function and fragmentation function is around 1.5 GeV, which for the present choice of α limits the pQCD calculation to $p_T > 3$ GeV. Nevertheless the effect of Q is predominantly a change in normalization of the pQCD prediction, and a larger value of α can be used to extrapolate the pQCD calculation to low p_T. We have verified that this approach provides a reasonable description of the available low p_T photon data from RHIC [66], which are available down to $p_T \approx 1$ GeV. This extrapolation scheme is thus used to estimate the prompt photon signal at low p_T in $p+p$ and $p+A$ collisions.

Figure 2 shows the direct photon spectra and p_T-differential elliptic and triangular flow coefficients in 0%–1% $p+\mathrm{Pb}$ collisions at 5.02 TeV. In order to calculate the prompt photon spectrum, the number of binary

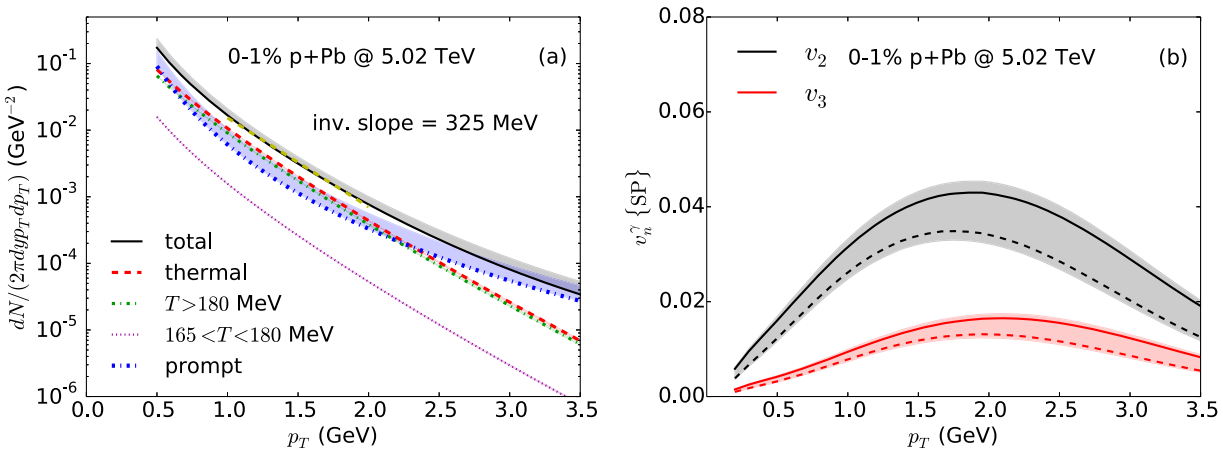

FIG. 2. (a) Direct photon spectra and (b) $v_n^\gamma\{\mathrm{SP}\}$ from 0%–1% $p+\mathrm{Pb}$ collisions at $\sqrt{s} = 5.02$ TeV. The shaded bands indicate the theoretical uncertainty in determining N_{coll} from the MCGlb model as explained in the main text. In panel (a), the inverse slope of the direct photon spectra is obtained from fitting the inverse slope in the range $p_T \in [1.0, 2.0]$ GeV.

collisions $N_{\rm coll}$ is required. Since binary scaling is known to be difficult to estimate for ultracentral $p+A$ events, we consider two values of $N_{\rm coll}$ and define their difference as the uncertainty inherent in the prompt photon calculation. One value of $N_{\rm coll}$ is calculated with our MCGlb model (listed in Table I) and a larger one, $N_{\rm coll}=26.1$, is estimated using the Glauber-Gribov model (with $\Omega=1.01$) from the ATLAS collaboration [67]. Note that high-p_T photon measurements for ultracentral events could help to reduce the uncertainty in $N_{\rm coll}$. Using this prescription for prompt photons, one finds that thermal photons emitted from the hot and dense medium outshine the prompt photon background by a factor of 2–3, for $p_T^\gamma \leq 2.5$ GeV. We reiterate that this result is obtained by only considering thermal photons emitted above $T=165$ MeV: If radiation emission below this temperature were also included, the thermal enhancement could be even larger (e.g., ~7% if the kinetic freeze out temperature is 105 MeV).

Two factors explain the large thermal photon signal in these small systems. First, the temperatures reached in the most central $p+$Pb collisions are considerably higher than the ones reached in peripheral Pb + Pb collisions, and is comparable to, or even larger than, the temperatures reached in central Pb + Pb collisions. Second, the number of binary collisions in $p+$Pb collisions is much smaller than the one in Pb + Pb collisions. This last factor reduces the background signal from the prompt photon component, while the first increases the thermal photon production.

Importantly, the significant blueshift from hydrodynamic radial flow and the high temperatures reached at the early stages of the collision result in an inverse slope of 325 MeV for the direct photon spectrum, which is harder than the one measured in 0%–40% Pb + Pb collisions [23].

Figure 2(b) shows the anisotropic flow coefficients of direct photons in $p+$Pb collisions. The dashed lines represent results obtained with the prompt photons estimated with the $N_{\rm coll}$ from the ATLAS Glauber-Gribov model [67]. The bands represent the uncertainty in prompt photon production discussed previously, and also include the statistical error in thermal photon production from a finite number of hydrodynamical calculations. Unlike the situation in nucleus-nucleus collisions, in $p+$Pb events the direct photon anisotropic flow is seeded by the density fluctuations of the initial state. We find that the direct photons $v_{2,3}\{\mathrm{SP}\}(p_T)$ have roughly the same sizes compared to 0%–40% centrality in Pb + Pb collisions [41,56]. Despite the short fireball lifetime in central $p+$Pb collisions (~4 fm/c), the system develops anisotropic flow quickly because of the large pressure gradients. Because this large anisotropy of direct photons is generated during the collective expansion of the fireball, the measurement of photon flow observables can provide an independent validation of hydrodynamics in environments with small volumes and large pressure gradients. A global analysis with hadronic observables can therefore lead to tight constraints on the transport properties of the QGP.

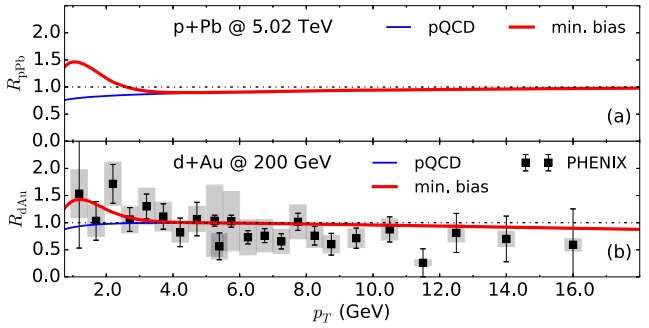

FIG. 3. The nuclear modification factor for direct photons in minimum bias $p+$Pb collisions at 5.02 TeV (a) and $d+$Au collisions at 200 GeV (b) [66]. The calculations of prompt photon emission include isospin and shadowing corrections.

As photon production in highly central collisions of light-heavy ions has yet to be measured, we estimate the thermal component in the nuclear modification factor $R_{p\rm Pb}$ and $R_{d\rm Au}$ for direct photons in minimum bias collisions in Fig. 3, and compare with existing data at RHIC. By including the thermal radiation component, we find a sizable enhancement of $R_{p\rm Pb}$ and $R_{d\rm Au}$ over the prompt baseline [61] for $p_T<3$ GeV. The thermal photon radiation leaves a clear and robust measurable signal in the minimum bias measurement. Our results for $d+$Au collisions at 200 GeV are consistent with the current PHENIX measurements [66]. A reduction of the uncertainties in the experimental data at the low p_T has the potential to distinguish the pure prompt production scenario from one with additional thermal radiation. For $p+$Pb collisions at 5.02 TeV, the signal of the thermal enhancement is more pronounced than the one at RHIC energy. The nuclear modification factor is however roughly the same, owing to a smaller prompt photon R_{pA} at the LHC [61]. The observation of such an enhancement in the direct photon nuclear modification factor can serve as a possible signature of the existence of quark-gluon plasma in small collision systems. Note that considering the inclusion of thermal photon radiation in minimum bias pp collisions (but perhaps going beyond the validity of hydrodynamics), $R_{\rm pPb}$ will be reduced by at most 20% for $p_T<1.5$ GeV.

Conclusions.—In this Letter, we propose to use direct photons as a signature of the existence of the hot quark-gluon plasma in the $d+$Au and $p+$Pb collisions at the RHIC and the LHC. Owing to compact fireball sizes, these systems can achieve high temperatures, comparable with those in central Pb + Pb collisions. Compared to $A+A$ collisions, a smaller number of binary collisions reduces the background of prompt photons. These two factors cause the thermal photon signal to shine over its prompt counterpart in high multiplicity events. Future work will consider evolution in three spatial dimensions [68] necessary for

asymmetric systems where boost invariance may not be a good approximation, the presence of a semi-QGP [32], the introduction of an IP-Glasma initial state [69], a possible hard photon component [70], and the inclusion of a coefficient of bulk viscosity [56,58]. We predict that the anisotropic flow of direct photons in $p+\mathrm{Pb}$ collisions will be comparable to those measured in $\mathrm{Pb}+\mathrm{Pb}$ collisions. It is found that the thermal photon radiation can also leave a measurable trace in minimum bias $d+\mathrm{Au}$ and $p+\mathrm{Pb}$ collisions at the RHIC and at the LHC. Precise measurements of direct photon spectra at low p_T have the potential to reveal the quark-gluon plasma formed in these light-heavy ion collisions. Moreover, the consequences of a low p_T thermal photon signal in small system collisions must be taken into account if direct photon measurements from such collisions are used to constrain cold nuclear matter effects.

The authors thank Friederike Bock for useful discussions. This work was supported by the Natural Sciences and Engineering Research Council of Canada. G. S. Denicol acknowledges support through a Banting Fellowship of the Natural Sciences and Engineering Research Council of Canada. Computations were made on the Guillimin supercomputer at McGill University, managed by Calcul Québec and Compute Canada. The operation of this supercomputer is funded by the Canada Foundation for Innovation (CFI), Ministère de l'Économie, de l'Innovation et des Exportations du Québec (MEIE), RMGA and the Fonds de recherche du Québec—Nature et technologies (FRQ-NT).

[1] C. Gale, S. Jeon, and B. Schenke, Int. J. Mod. Phys. A **28**, 1340011 (2013).
[2] U. Heinz and R. Snellings, Annu. Rev. Nucl. Part. Sci. **63**, 123 (2013).
[3] B. Abelev *et al.* (ALICE Collaboration), Phys. Lett. B **719**, 29 (2013).
[4] S. Chatrchyan *et al.* (CMS Collaboration), Phys. Lett. B **718**, 795 (2013).
[5] G. Aad *et al.* (ATLAS Collaboration), Phys. Rev. Lett. **110**, 182302 (2013).
[6] A. Adare *et al.* (PHENIX Collaboration), Phys. Rev. Lett. **111**, 212301 (2013).
[7] V. Khachatryan *et al.* (CMS Collaboration), Phys. Rev. Lett. **115**, 012301 (2015).
[8] B. B. Abelev *et al.* (ALICE Collaboration), Phys. Lett. B **726**, 164 (2013).
[9] V. Khachatryan *et al.* (CMS Collaboration), Phys. Lett. B **742**, 200 (2015).
[10] A. Adare *et al.* (PHENIX Collaboration), Phys. Rev. Lett. **114**, 192301 (2015).
[11] A. Dumitru, K. Dusling, F. Gelis, J. Jalilian-Marian, T. Lappi, and R. Venugopalan, Phys. Lett. B **697**, 21 (2011).
[12] K. Dusling and R. Venugopalan, Phys. Rev. D **87**, 051502 (2013).
[13] K. Dusling and R. Venugopalan, Phys. Rev. D **87**, 094034 (2013).
[14] A. Dumitru, L. McLerran, and V. Skokov, Phys. Lett. B **743**, 134 (2015).
[15] J. L. Nagle, A. Adare, S. Beckman, T. Koblesky, J. O. Koop, D. McGlinchey, P. Romatschke, J. Carlson, J. E. Lynn, and M. McCumber, Phys. Rev. Lett. **113**, 112301 (2014).
[16] P. Bozek, Phys. Rev. C **85**, 014911 (2012).
[17] P. Bozek and W. Broniowski, Phys. Lett. B **718**, 1557 (2013).
[18] B. Schenke and R. Venugopalan, Phys. Rev. Lett. **113**, 102301 (2014).
[19] K. Werner, M. Bleicher, B. Guiot, I. Karpenko, and T. Pierog, Phys. Rev. Lett. **112**, 232301 (2014).
[20] I. Kozlov, M. Luzum, G. Denicol, S. Jeon, and C. Gale, arXiv:1405.3976.
[21] See for example, C. Gale, Landolt-Bornstein **23**, 445 (2010), and references therein, DOI: 10.1007/978-3-642-01539-7_15.
[22] A. Adare *et al.* (PHENIX Collaboration), Phys. Rev. Lett. **104**, 132301 (2010).
[23] M. Wilde (ALICE Collaboration), Nucl. Phys. **A904–905**, 573c (2013).
[24] A. Adare *et al.* (PHENIX Collaboration), Phys. Rev. Lett. **109**, 122302 (2012).
[25] A. Adare *et al.* (PHENIX Collaboration), Phys. Rev. C **91**, 064904 (2015).
[26] B. Bannier (PHENIX Collaboration), Nucl. Phys. **A931**, 1189 (2014).
[27] D. Lohner (ALICE Collaboration), J. Phys. Conf. Ser. **446**, 012028 (2013).
[28] M. Dion, J. F. Paquet, B. Schenke, C. Young, S. Jeon, and C. Gale, Phys. Rev. C **84**, 064901 (2011).
[29] J. Ghiglieri, J. Hong, A. Kurkela, E. Lu, G. D. Moore, and D. Teaney, J. High Energy Phys. 05 (2013) 010.
[30] C. Shen, J. F. Paquet, U. Heinz, and C. Gale, Phys. Rev. C **91**, 014908 (2015).
[31] M. Heffernan, P. Hohler, and R. Rapp, Phys. Rev. C **91**, 027902 (2015).
[32] C. Gale, Y. Hidaka, S. Jeon, S. Lin, J.-F. Paquet, R. D. Pisarski, D. Satow, V. V. Skokov, and G. Vujanovic, Phys. Rev. Lett. **114**, 072301 (2015).
[33] H. van Hees, C. Gale, and R. Rapp, Phys. Rev. C **84**, 054906 (2011).
[34] H. van Hees, M. He, and R. Rapp, Nucl. Phys. **A933**, 256 (2015).
[35] R. Chatterjee, H. Holopainen, T. Renk, and K. J. Eskola, Phys. Rev. C **83**, 054908 (2011).
[36] R. Chatterjee, H. Holopainen, I. Helenius, T. Renk, and K. J. Eskola, Phys. Rev. C **88**, 034901 (2013).
[37] O. Linnyk, V. P. Konchakovski, W. Cassing, and E. L. Bratkovskaya, Phys. Rev. C **88**, 034904 (2013).
[38] O. Linnyk, W. Cassing, and E. L. Bratkovskaya, Phys. Rev. C **89**, 034908 (2014).
[39] C. Shen, J. F. Paquet, J. Liu, G. Denicol, U. Heinz, and C. Gale, Nucl. Phys. **A931**, 675 (2014).
[40] C. Shen, U. W. Heinz, J. F. Paquet, and C. Gale, Phys. Rev. C **89**, 044910 (2014).
[41] C. Shen, U. W. Heinz, J. F. Paquet, I. Kozlov, and C. Gale, Phys. Rev. C **91**, 024908 (2015).
[42] O. Linnyk, V. Konchakovski, T. Steinert, W. Cassing, and E. L. Bratkovskaya, Phys. Rev. C **92**, 054914 (2015).

[43] C. Shen, Z. Qiu, H. Song, J. Bernhard, S. Bass, and U. Heinz, Comput. Phys. Commun. **199**, 61 (2016).
[44] S. Chatrchyan *et al.* (CMS Collaboration), Phys. Lett. B **724**, 213 (2013).
[45] L. Hulthén and M. Sagawara, *Handbuch der Physik*, edited by S. Flügge (Springer-Verlag, New York, 1957), Vol. 39.
[46] B. Alver, M. Baker, C. Loizides, and P. Steinberg, arXiv:0805.4411.
[47] S. S. Adler *et al.* (PHENIX Collaboration), Phys. Rev. C **77**, 014905 (2008).
[48] M. Alvioli, H.-J. Drescher, and M. Strikman, Phys. Lett. B **680**, 225 (2009).
[49] M. Alvioli, H. Holopainen, K. J. Eskola, and M. Strikman, Phys. Rev. C **85**, 034902 (2012).
[50] H. Song and U. W. Heinz, Phys. Rev. C **77**, 064901 (2008).
[51] P. Huovinen and P. Petreczky, Nucl. Phys. **A837**, 26 (2010).
[52] H. Niemi, G. S. Denicol, P. Huovinen, E. Molnar, and D. H. Rischke, Phys. Rev. Lett. **106**, 212302 (2011).
[53] H. Niemi and G. S. Denicol, arXiv:1404.7327.
[54] P. B. Arnold, G. D. Moore, and L. G. Yaffe, J. High Energy Phys. 12 (2001) 009.
[55] S. Turbide, R. Rapp, and C. Gale, Phys. Rev. C **69**, 014903 (2004).
[56] J. F. Paquet, C. Shen, G. S. Denicol, M. Luzum, B. Schenke, S. Jeon, and C. Gale, arXiv:1509.06738.
[57] S. Chatrchyan *et al.* (CMS Collaboration), Eur. Phys. J. C **74**, 2847 (2014).
[58] S. Ryu, J.-F. Paquet, C. Shen, G. S. Denicol, B. Schenke, S. Jeon, and C. Gale, Phys. Rev. Lett. **115**, 132301 (2015).
[59] P. Aurenche, R. Baier, M. Fontannaz, and D. Schiff, Nucl. Phys. **B297**, 661 (1988).
[60] F. Aversa, P. Chiappetta, M. Greco, and J. P. Guillet, Nucl. Phys. **B327**, 105 (1989).
[61] I. Helenius, K. J. Eskola and H. Paukkunen, J. High Energy Phys. 05 (2013) 030.
[62] K. J. Eskola, H. Paukkunen, and C. A. Salgado, J. High Energy Phys. 04 (2009) 065.
[63] D. Stump, J. Huston, J. Pumplin, W. K. Tung, H. L. Lai, S. Kuhlmann, and J. F. Owens, J. High Energy Phys. 10 (2003) 046.
[64] L. Bourhis, M. Fontannaz, and J. P. Guillet, Eur. Phys. J. C **2**, 529 (1998).
[65] J.-F. Paquet, MSc thesis, McGill University, 2011.
[66] A. Adare *et al.*, Phys. Rev. C **87**, 054907 (2013).
[67] The ATLAS Collaboration, Report Nos. ATLAS-CONF-2013-096, ATLAS-COM-CONF-2013-117.
[68] B. Schenke, S. Jeon, and C. Gale, Phys. Rev. C **82**, 014903 (2010).
[69] B. Schenke, P. Tribedy, and R. Venugopalan, Phys. Rev. Lett. **108**, 252301 (2012); Phys. Rev. C **86**, 034908 (2012).
[70] L. McLerran and B. Schenke, Nucl. Phys. **A946**, 158 (2016).